Journal of Molecular Catalysis A: Chemical 300 (2009) 80–88

Contents lists available at ScienceDirect

Journal of Molecular Catalysis A: Chemical

journal homepage: www.elsevier.com/locate/molcata

Characteristics of Au/Mg_xAlO hydrotalcite catalysts in CO selective oxidation

Ching-Tu Chang[a,c], Biing-Jye Liaw[b], Yu-Pei Chen[c], Yin-Zu Chen[a,*]

[a] Department of Chemical and Materials Engineering, National Central University, Jhongli 32001, Taiwan, ROC
[b] Department of Chemical and Materials Engineering, Nanya Institute of Technology, Jhongli 32091, Taiwan, ROC
[c] Institute of Nuclear Energy Research Atomic Energy Council, Longtan 32546, Taiwan, ROC

ARTICLE INFO

Article history:
Received 27 February 2008
Available online 5 November 2008

Keywords:
CO selective oxidation
Catalyst preparation
Gold catalysts
Hydrotalcite
Mg_xAlO

ABSTRACT

Gold catalysts, supported on a solid base of Mg_xAlO hydrotalcite, were prepared by a modified deposition precipitation method for CO selective oxidation. The preparation parameters and pretreatment of the catalysts were investigated. The pH and the $HAuCl_4$ concentration in the initial solution, and the Mg/Al molar ratio of Mg_xAlO affected the pH in the final solution and determined the actual gold loading of the catalyst. The calcination temperatures of the Mg_xAlO support and the Au/Mg_xAlO catalyst dominated the Au^{3+}/Au^0 ratio on the catalyst. The pretreatment of the catalyst as well as the gold loading and the Au^{3+}/Au^0 ratio, critically determined the activity of the catalyst for CO selective oxidation. Based on XPS and in situ DR-FTIR analyses, a mechanism for CO selective oxidation on 2%Au/Mg_2AlO was proposed. The hydroxyl group on Mg_2AlO also participated in the reaction.

1. Introduction

In the last decade, CO oxidation and selective CO oxidation in excess hydrogen over gold catalysts at low temperature were extensively studied [1–5]. The activity of the supported gold catalyst in CO oxidation at low temperature depends on various factors. Generally, the size of Au particles [6], the nature of supports, the preparation methods [7–11], the preparation parameters and the pretreatment conditions [12–17] affect the performance of the gold catalysts. To date, explanations for the activities of gold catalysts have focused mainly on the size of the Au particles [18,19] and the nature of the support material [20–22], including electronic quantum-size effects, strain and oxygen diffusion via the support, as well as the oxidation state of the gold particles [23–25]. Additionally, support materials can affect the reactivity and are categorized as active (TiO_2, Fe_2O_3, CeO_2, MnO) or inactive (SiO_2, MgO, Al_2O_3) [26]. Active supports can provide oxygen atoms and thus enhance activity; moreover, they are also capable of enhancing the stability of small gold particles. The reactivity of gold clusters on inactive supports is attributed to the high dispersion of the metal and the presence of a low-coordinated gold surface site [6,27]. Hodge et al. [28] utilized Mössbauer spectroscopy to conclude that the most active catalyst has an Au^{3+}/Au^0 ratio of approximately 3/2. Based on XPS and EXAFS analyses, Park and Lee [29] proposed that the oxidized gold is the active species in gold catalyst supported on TiO_2, Al_2O_3 and Fe_2O_3. Visco et al. [30] found that the uncalcined samples were much more active than the calcined ones, and proposed that oxidized gold species constitute the major active sites for CO oxidation at low temperature. Date and Haruta [31] claimed that a good catalyst of CO oxidation requires the co-existence of metallic and cationic gold states. Nevertheless, the role of Au^{3+}/Au^0 is still a matter of controversy. The involvement of hydroxyl groups on Au^{x+} or supports in CO oxidation was proposed over the gold catalysts supported on Fe_2O_3 [28] and MgO [32]. Date et al. [33] proposed the role of moisture on the activation of oxygen on the support and the decomposition of carbonate intermediate on the gold catalyst.

The deposition precipitation (DP) method developed by Haruta's group [34] has been extensively applied to prepare gold catalysts for CO oxidation. In this procedure, the iso-electric point (IEP) of the support is critical for the deposition of gold species. The surface of a transition metal oxide is typically charged because of its amphoteric character and the dissociation of the OH group on it. The positive and negative charges on the surface are compensated for each other at the IEP. If the pH in the solution is lower than the pH of IEP, the surface is positively charged and anion adsorption occurs. On the other hand, if the pH in the solution is higher than the pH of IEP, the surface is negatively charged and will adsorb only cations. The oxides with an IEP of approximately 7, including CeO_2 (IEP = 6.75) [35], Fe_2O_3 (IEP = 6.5–6.9) [34], TiO_2 (IEP = 6), and ZrO_2 (IEP = 6.7) [36] have been extensively used as supports to obtain an active catalyst, while an acidic support such as SiO_2 (IEP = 1–2) [13] or a basic support such as Mg_xAlO (IEP = 10) [14], MgO (IEP = 12) [37] is not typically used as a support. Al_2O_3, an amphoteric oxide (IEP = 8) has been reported to generate either an active or even inactive gold catalyst [38]. MgO is well known for stabilizing the nano-sized particles of gold on it [39] and Mg_xAlO has a similar property [7]. No

* Corresponding author. Tel.: +886 3 4227151; fax: +886 3 4252296.
E-mail address: ynzuchen@cc.ncu.edu.tw (Y.-Z. Chen).

1381-1169/$ – see front matter © 2008 Elsevier B.V. All rights reserved.
doi:10.1016/j.molcata.2008.10.040

suitable method was proposed to obtain an active gold catalyst on a solid base of MgO [11] or Mg_xAlO [14]. In our recent study, the solid base of Mg_xAlO hydrotalcite was used as a support to elucidate an optimal method of obtaining an active catalyst for CO oxidation [7].

Mg_xAlO hydrotalcite compounds are double-layered hydroxides, and consist of positively charged metal hydroxide layers that are separated from each other by anions and water molecules. The layers contain metal cations of at least two different oxidation states [40]. The structure of hydrotalcite is similar to that of brucite, $Mg(OH)_2$. The hydrotalcites are commonly utilized as catalysts or catalyst precursors, ion exchangers, adsorbents, and polymer stabilizers and for other purposes [41,42]. The objective of this study is to use the solid base of Mg_xAlO hydrotalcite to stabilize the nano-sized particles of gold on it for CO selective oxidation and determine the factors, apart from particle size, that govern the catalysis of gold. In this investigation, Mg_xAlO hydrotalcites with various Mg/Al molar ratios were prepared by co-precipitation, and gold catalysts containing 2 wt% Au (2%Au/Mg_xAlO) was prepared by DP. The effect of various parameters on the preparation, and pretreatment of Au/Mg_xAlO catalysts for CO selective oxidation were studied. The XPS and in situ DR-FTIR analyses were used to discuss the role of surface hydroxyls on Au/Mg_xAlO catalysts.

2. Experimental

2.1. Preparation of support and catalyst

The hydrotalcite supports of Mg_xAlO (x = Mg/Al molar ratio) were prepared by co-precipitation of an aqueous solution of magnesium and aluminum salts with a highly basic carbonate solution. The salt solution (1 M) contained $Mg(NO_3)_2{\cdot}6H_2O$ and $Al(NO_3)_3{\cdot}9H_2O$ dissolved in deionized water at various Mg/Al molar ratios (x = 1–4). The basic solution of equal volume contained KOH and K_2CO_3 in the molar ratios of $CO_3^{2-}/(Al+Mg) = 0.67$ and $OH^-/(Al+Mg) = 2.25$. These two solutions were mixed at 60 ml/h, with a constant pH of approximately 10 maintained, and then aged overnight with stirring. The white precipitate was washed, dried at 100 °C, and then calcined in air at various temperatures (200–475 °C). The resulting hydrotalcite supports were designated as $Mg_xAlO(T)$, in which x was the Mg/Al molar ratio and T was the calcination temperature of support.

The catalysts were prepared by the Haruta's DP method [34] and a modified DP method [7]. In the typical DP method, the pH in the initial $HAuCl_4$ solution (pH_i) was first adjusted to 4–9 by using 0.5 M $NaCO_3$ solution. In the modified method, the pH of approximately 2 in the initial solution (pH_i 2) was not changed. The hydrotalcite support of $Mg_xAlO(T)$ was first well dispersed in 100 ml of water, and then the mixture was poured into the gold solution slowly at a speed of approximately 3 ml/min for deposition precipitation at 70 °C. The obtained catalyst precursor was aged at 70 °C for 3 h, and then washed and dried overnight at 100 °C. The catalysts were calcined at various temperatures (100–500 °C) for 4 h.

2.2. Characterization of catalysts

The specific surface areas (S_{BET}) of the samples were determined by nitrogen adsorption with a Micromeritics ASAP-2020 apparatus at −196 °C following degassing at 100 °C. The compositions of the sample were identified by inductively coupled plasma analysis (ICP) using a Jobin JY-24 device. X-ray diffraction (XRD) patterns were obtained using a Siemens-500 diffractometer with Cu Kα radiation (λ = 0.1542 nm).

Transmission electron microscopy (TEM) photographs were taken using a JEOL JEM-2999FMII apparatus. Samples for TEM study were prepared by gently grinding a catalyst to powder in a mortar; the synthesized powder was ultrasonically dispersed in ethanol. The solution was deposited onto a carbon-coated Cu mesh grid, by using a pipette, and then naturally evaporating the solvent. The mean particle diameters were determined by counting ~150 particles in the enlarged photographs.

The X-ray photoelectron spectroscopy (XPS) measurements were made using a Thermo VG Scientific Sigma Prob spectrophotometer with Al Kα radiation (1486.6 eV). The nanoparticles were first pressed into a 10 mm × 10 mm disk and immediately transferred to the pretreatment chamber after fixing onto the sample holder. In the chamber, each sample was degassed overnight at 1×10^{-6} Torr to remove the volatile contaminants and was then transferred to the analyzing chamber for XPS analysis. The spectra were obtained at an analyzer pass energy of 25.5 eV and an electron take-off angle of 45°. The vacuum in the test chamber was maintained below 1.33×10^{-8} Torr during the collection. Binding energies were corrected for surface charging by referencing them to the energy of the C 1s peak of the contaminant carbon at 284.6 eV.

Diffuse reflection Fourier transform infrared spectroscopy (DR-FTIR) was performed using a Varian 3100 FTIR with Varian software. The sample was first treated in flowing He at 100 or 300 °C for 3 h before each experiment. The heating rate during the treatment was 10 °C/min. Then, the sample was cooled under He to an operation temperature of either 25 or 70 °C. Infrared spectra were recorded against a background of the sample at the reaction under flowing He. IR spectra were recorded with the co-addition of 300 scans in single beam spectra or absorbance spectra, at a resolution of 4 cm^{-1}. The catalyst was then exposed to CO, or a mixture of CO and O_2 in He. The total flow rate was 50 ml/min, set by Brooks 5850 mass flow controllers.

2.3. Selective CO oxidation (SCO)

A total of 100 mg of catalyst was loaded into a tubular stainless-steel reactor with an internal diameter of 8 mm and a length of 500 mm. The reactor was placed in a three-sectional temperature-controlled oven. The catalysts were placed in a quartz tube and secured between two quartz wool plugs. The composition of the reactant gas was typically $H_2/CO/O_2/He$ (50/1/1/48). This gaseous mixture was allowed to flow to the reactor at a flow rate of 100 ml/min (F/W = 60,000 ml/(g h)) using Brooks 5850 mass flow controllers. The reaction temperature was increased stepwise from room temperature to 120 °C. CO and O_2 were analyzed using a gas chromatograph equipped with a 1/8-in. × 15 ft 60/80 Carboxen-1000 column (SUPELCO) and a TCD detector.

3. Results and discussion

In our earlier work [7], a modified Haruta's DP method was adopted to prepare the Au catalysts, which were supported on the solid base-Mg_xAlO hydrotalcite, for CO oxidation. The oxidation of CO on Au/Mg_xAlO catalysts is very sensitive to the preparation parameters. 2%Au/Mg_xAlO catalysts prepared with various parameters were used to evaluate their effectiveness in the selective CO oxidation in hydrogen-rich gas. The activation of 2%Au/Mg_xAlO catalysts during SCO was observed and the behaviors of Mg_xAlO were discussed.

3.1. Effect of preparation parameters

Fig. 1 displays CO selective oxidation over 2%Au/Mg_2AlO catalysts prepared at various pH_i in the initial $HAuCl_4$ solution. Among these catalysts with Au particles of similar sizes (3.6–3.8 nm), 2%Au/Mg_2AlO prepared without adjusting the pH (pH_i 2) of the

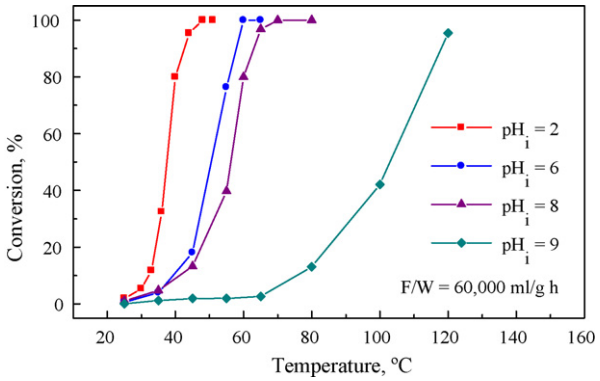

Fig. 1. Effect of gold solution pH_i on CO selective oxidation over 2%Au/Mg_2AlO catalysts.

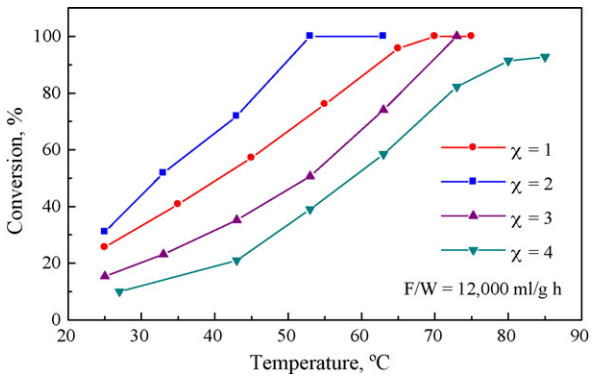

Fig. 3. Effect of Mg/Al molar ratio on CO selective oxidation over 2%Au/Mg_xAlO catalysts.

initial solution was the most active. The actual loadings of the 2%Au/Mg_2AlO catalysts that corresponded to pH_i 2, 6, 8 and 9 were 1.2%, 0.86%, 0.8% and 0.48%, respectively. The activities declined markedly as the pH_i increased, which result was consistent with the real loadings of gold. Mg_xAlO, a well-known solid base [14], increases the pH of the $HAuCl_4$ solution from 2 (pH_i) to about 7.2 (pH_f). Generally, a $HAuCl_4$ solution with a pH of about 7 is optimal for the deposition of gold complex species of $[AuCl(OH)_3]^-$ and $[Au(OH)_4]^-$ on the positively charged supports [15]. This modified DP method was used to prepare Au/Mg_xAlO catalysts without adjusting the pH of the initial gold solution and is described as follows.

Fig. 2 shows the extent of CO selective oxidation over the 2%Au/Mg_2AlO catalysts that are prepared in the $HAuCl_4$ solution at various concentrations. The 2%Au/Mg_2AlO catalyst prepared at a concentration of 1×10^{-3} M was most active. The actual loadings of the 2%Au/Mg_2AlO catalysts prepared at 1×10^{-3}, 7×10^{-4} and 5×10^{-4} M were 1.2%, 1.06% and 0.75%, respectively [7]. The activities of the catalysts increased with the concentration of $HAuCl_4$, which result was also consistent with the actual gold loadings. Although the 2%Au/Mg_2AlO catalyst prepared at 1×10^{-2} M had a larger gold loading (1.8%) than that prepared at 1×10^{-3} M, it did not exhibit greater activity. The gold complex species in the gold solution at 1×10^{-2} M have more chlorine ligands than at 1×10^{-3} M, reducing the reactivity of the formed catalyst. As for gold catalysts, 1×10^{-3} M is the optimal concentration for the preparation of gold catalysts by the DP method [7,50].

Fig. 3 displays CO selective oxidation over the 2%Au/Mg_xAlO catalysts that were prepared with various molar Mg/Al ratios. The 2%Au/Mg_2AlO catalyst with Mg/Al = 2 had the lowest starting temperature for CO selective oxidation. The activity decreased markedly as the Mg/Al ratio increased. All Mg_xAlO (x = 1–4) have the same typical structure of hydrotalcite and similar surface areas, but their basic strengths are different. As stated elsewhere, the basic strength of Mg_xAlO increased with the Mg/Al ratio [43]. The pH values of the final solutions were 7.0, 7.2, 8.2 and 8.4 for Mg_xAlO with x = 1, 2, 3 and 4, respectively. The actual loadings of gold for 2%Au/Mg_xAlO with x = 3, 4 were much lower than those of 2%Au/Mg_xAlO with x = 1, 2. The pH values of the final solution determined the actual loading of the gold catalyst and the activity in CO selective oxidation.

3.2. Effect of calcination temperature of Mg_2AlO support and catalyst on CO selective oxidation

Fig. 4 shows CO selective oxidation over the Au/$Mg_2AlO(T)$ catalysts with $Mg_2AlO(T)$ calcined at various temperatures (100–475 °C). 2%Au/$Mg_2AlO(100)$ with Mg_2AlO calcined at 100 °C was the most active catalyst. The higher calcination temperature of $Mg_2AlO(T)$ was associated with the lower activity of the 2%Au/$Mg_2AlO(T)$ catalyst. The 2%Au/$Mg_2AlO(T)$ catalysts have considerable loadings (1.05–1.20 wt%) and similar particle sizes (3.6–3.8 nm), so the loading was not the major factor that determined the activity, as in the foregoing discussions. The relative proportions of the gold states were estimated by the deconvolution of the Au 4f peaks in the XPS spectra, as displayed in Fig. 5 and Table 1. The 2%Au/$Mg_2AlO(100)$ catalyst had the largest Au^{3+}/Au^0 ratio, which was about 1.2. As the calcination temperature of Mg_2AlO increased, the Au^{3+}/Au^0 ratio declined. The activity declined markedly as the Au^{3+}/Au^0 ratio decreased from 1.19 to 0.64. Just as for CO oxidation, as described elsewhere [7], the

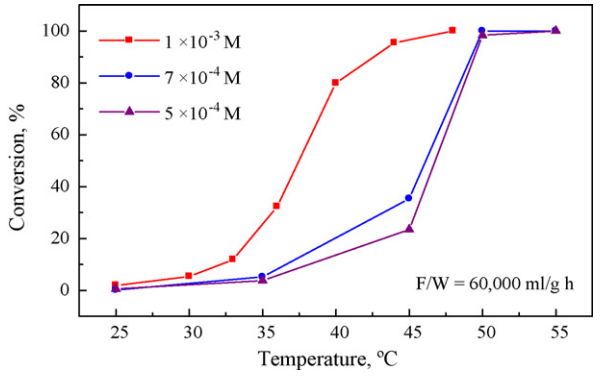

Fig. 2. Effect of the $HAuCl_4$ concentration in the initial solution on CO selective oxidation over 2%Au/Mg_2AlO catalyst.

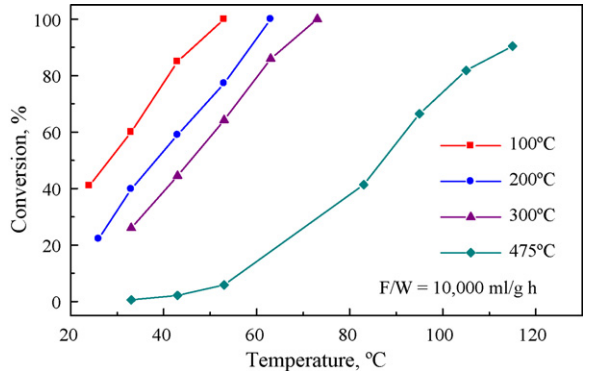

Fig. 4. Effect of calcination temperature of Mg_2AlO support on CO selective oxidation over 2%Au/Mg_2AlO catalysts.

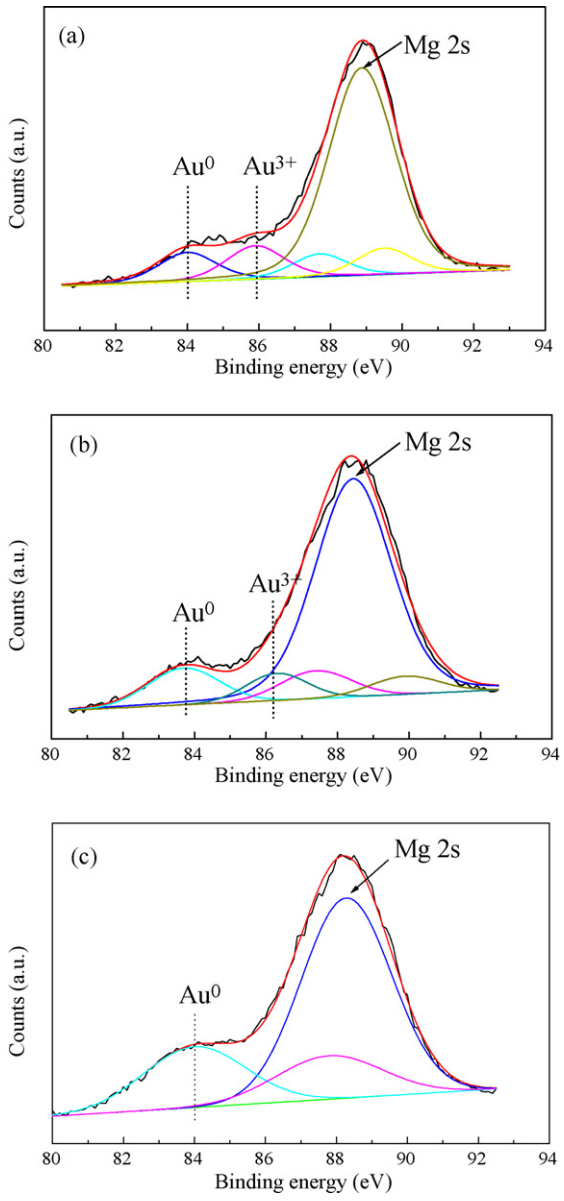

Fig. 5. XPS spectra of Au 4f for 2%Au/$Mg_2AlO(T)$ calcined at 100 °C (a), 475 °C (b) and 2%Au/$Mg_2AlO(100)$ catalyst calcined at 300 °C (c).

Au^{3+}/Au^0 ratio was the dominant factor in affecting the performance of the 2%Au/$Mg_2AlO(T)$ catalysts in CO selective oxidation.

Fig. 6 plots the extent of CO selective oxidation over the 2%Au/$Mg_2AlO(100)$ catalysts calcined at 100 and 300 °C. The

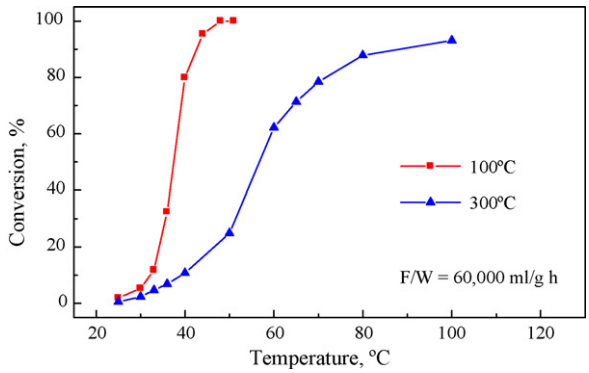

Fig. 6. Effect of calcination temperature of 2%Au/Mg_2AlO catalyst on CO selective oxidation.

Au^{3+}/Au^0 ratio was about 1.19 for the 2%Au/$Mg_2AlO(100)$ catalyst calcined at 100 °C (Table 1), and Au^{3+} was completely reduced to Au^0 when the catalyst was calcined at 300 °C (Fig. 5). TEM analysis revealed no significant agglomeration of gold particles as the calcination temperature was increased from 100 °C to 300 °C (Fig. 7). The activity of 2%Au/$Mg_2AlO(100)$ declined sharply as the calcination temperature increased to 300 °C, which result was consistent with the disappearance of the oxidized state of gold (Au^{3+}).

Fig. 8 displays the FTIR spectra of CO adsorbed on the 2%Au/$Mg_2AlO(100)$ catalysts that were calcined at 100 and 300 °C. The two absorption bands at 2116 and 2131 cm^{-1} observed on the sample calcined at 100 °C were assigned to CO adsorbed on Au^0 and Au^{3+}, respectively [44–47]. Only one dominant absorption band at 2112 cm^{-1}, assigned to Au^0, was observed on the 2%Au/$Mg_2AlO(100)$ catalyst calcined at 300 °C. The absorption band at 2170–2190 cm^{-1} is typically attributed to CO adsorbed on the support [44,45]. The absorption band at 2174 cm^{-1} could be assigned to CO adsorbed on the support of Mg_2AlO.

These results supported the assertion that the active sites involve an ensemble of metallic Au atoms and Au cations (Au^{3+} or Au^{1+}) [48,49]. A mechanism that involved the hydroxyl ligand on the Au cations for CO oxidation has been proposed [49]. The reaction proceeds by the insertion of an adsorbed CO into Au–OH to form a hydroxycarbonyl, which is oxidized by an adsorbed oxygen to form a bicarbonate, and is then decarboxylated to form Au–OH and CO_2.

Gold can be dispersed and stabilized on a solid base of Mg_xAlO hydrotalcite by a modified DP method, to obtain a good catalyst for CO oxidation [7] and CO selective oxidation. The optimal catalyst of 2%Au/Mg_2AlO was obtained with the preparation parameters as follows: (1) 1×10^{-3} M $HAuCl_4$, (2) pH 2 (without adjusting pH) of the initial solution, (3) Mg/Al = 2 (Mg_2AlO) calcined at 100 °C as a support, and (4) 2%Au/Mg_2AlO catalyst calcined at 100 °C. Just

Table 1
Surface composition of 2%Au/Mg_2AlO catalysts determined by the deconvolution of Au 4f peaks and comparison of their activity in CO selective oxidation.

Calcination temperature (°C)	Au^{3+}	Au^0	Au^{3+}/Au^0	Conversion, $T_{100\%}$ (°C)	Selectivity, S_{CO_2} (%)
Mg_2AlO supports[a]					
100	0.54	0.45	1.19	53	61.3
200	0.52	0.48	1.08	63	53.7
300	0.49	0.57	0.75	73	51.4
475	0.39	0.61	0.64	>110	<50
2%Au/Mg_2AlO catalysts[b]					
100	0.54	0.45	1.19	48	51
300	0.00	1.00	0.00	>100	<50
After SCO	0.60	0.40	1.50	25	81

[a] Calcination temperature of 2%Au/Mg_2AlO catalysts at 100 °C.
[b] Calcination temperature of Mg_2AlO support at 100 °C.

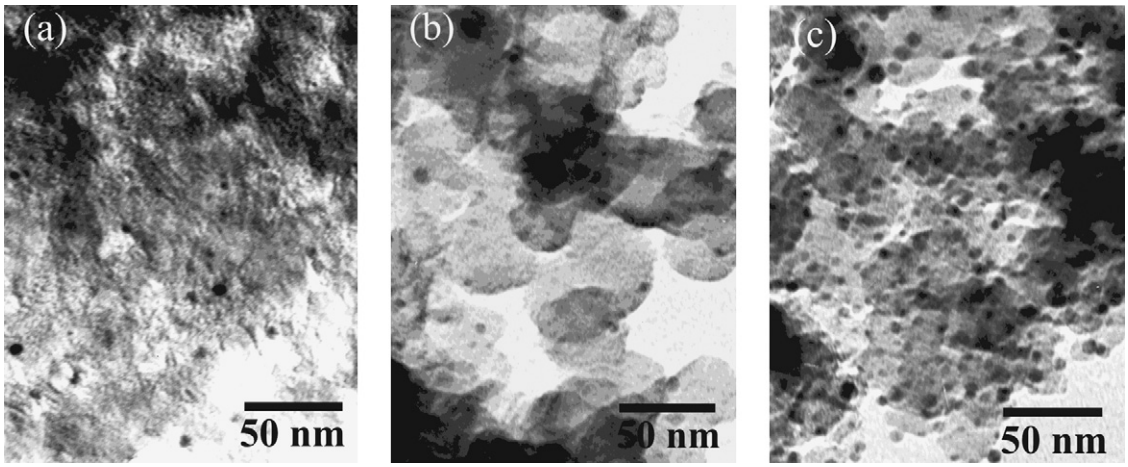

Fig. 7. TEM images of 2%Au/$Mg_2AlO(100)$ catalysts calcined at 100 °C (a), 200 °C (b), and 300 °C (c).

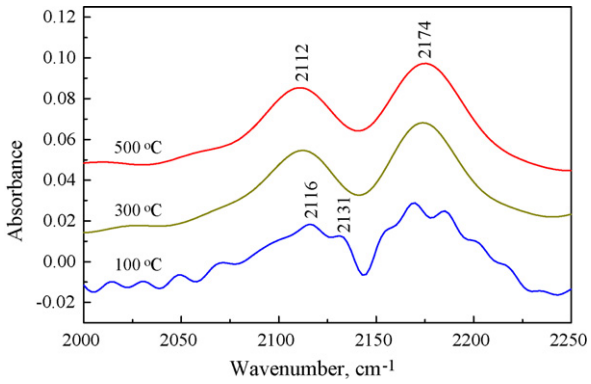

Fig. 8. In situ DR-FTIR spectra of the carbonyl region over 2%Au/Mg_2AlO under the stream of 10%CO/He (50 cm^3/min) at room temperature.

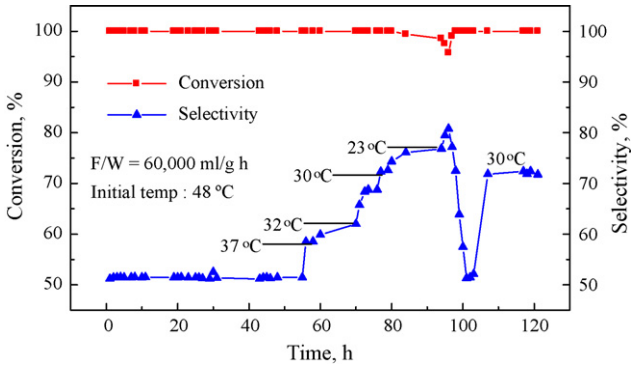

Fig. 10. Variation of the CO conversion and of the selectivity with the reaction time during the selective oxidation of CO. The reaction temperatures at each portion of the long time catalytic test are indicated alongside the small horizontal line.

like general gold catalysts, the selectivity of CO oxidation in excess hydrogen was about 50–60% at T_{100} of about 45 °C (Table 1).

3.3. *Effect of pretreatment on catalyst activity*

CO selective oxidation over 2%Au/Mg_2AlO catalyst during heating–cooling runs exhibited interesting characteristics, as displayed in Fig. 9. For the first run, the CO conversion increased with temperature, up to complete conversion at around 48 °C during heating, but the catalyst retained its activity upon complete conversion during cooling to room temperature, which was about 25 °C. Nevertheless, the selectivity increased from 51% to 81% during cooling. The 2%Au/Mg_2AlO catalyst retained its activity with complete conversion of CO during the repeated heating–cooling runs, as in Fig. 9, and even during the 120-h stability test, as displayed in Fig. 10.

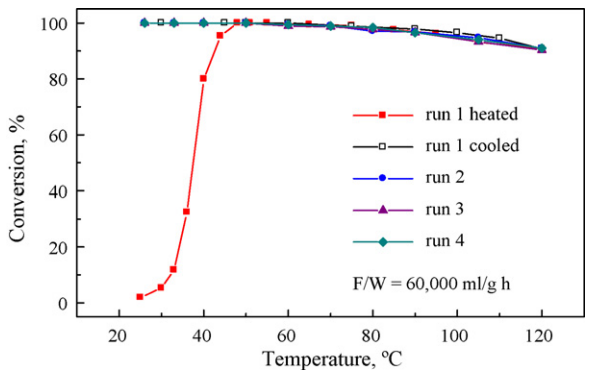

Fig. 9. Effect of the repeat operation through heated and cooled on the 2%Au/Mg_2AlO catalysts for the selective oxidation of CO.

Following CO selective oxidation, the 2%Au/Mg_2AlO catalyst was analyzed by TEM and XPS. No significant agglomeration of gold particles was observed, but the Au^{3+}/Au^0 ratio increased from 1.2 to 1.5. In the authors' earlier work on the CO oxidation the feed in the absence of H_2 [7], a fall-off hysteresis curve was obtained during cooling. It is worth noting the difference between the behavior of the 2%Au/Mg_2AlO catalyst in CO oxidation in the presence of H_2 and in the absence of H_2. It was speculated that H_2 or H_2O formed from the oxidation of H_2 could activate the 2%Au/Mg_2AlO catalyst. When 10%H_2/He, 1%H_2O/He and 10%H_2O/He were used to pretreat the 2%Au/Mg_2AlO catalyst at 60 °C, no activation was observed as shown in Fig. 11. Apparently, the high activity of catalyst resulted from the selective oxidation reaction, which is consistent with the in situ FTIR results for the catalysts pretreated at various pretreatment conditions (Fig. 12). The absorption band intensity of the hydroxyl group on 2%Au/$Mg_2AlO(100)$, pretreated with the selective oxidation conditions, was largest. However, similar and smaller intensities were obtained for 2%Au/$Mg_2AlO(100)$ pretreated under other conditions. Thus, the high activity of 2%Au/$Mg_2AlO(100)$ after the selective oxidation reaction might be attributed to the substantial increase in the hydroxyl group resulting from the formation and subsequent adsorption of H_2O onto the catalyst during the reaction. Date and Haruta [31] also noted the obvious influence of the amount of H_2O adsorbed on the catalyst during reaction on the

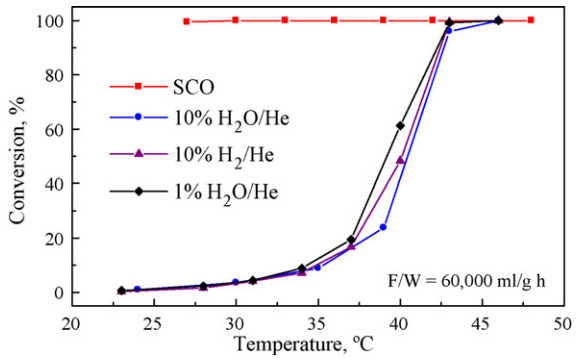

Fig. 11. Effect of the pretreatment condition on the 2%Au/Mg_2AlO catalysts for the selective oxidation of CO.

activity of the gold catalyst rather than the content of H_2O in the gas phase.

3.4. Fourier transform infrared spectroscopy (FTIR)

3.4.1. In situ DR-FTIR adsorption spectra of CO and CO/O_2

In situ DR-FTIR was performed to investigate the real-time adsorption of CO on the 2%Au/Mg_2AlO catalysts in a stream of 2%CO/He at room temperature. CO was first adsorbed on Mg_2AlO calcined at 100 and 300 °C to distinguish the adsorption properties of the Au atoms from those of the support materials. The 2%Au/Mg_2AlO(100) catalysts that were used to make the measurements were calcined at 100 and 300 °C in the presence or absence of O_2 to investigate the active sites of Au.

Fig. 13(a) and (b) displays the in situ DR-FTIR spectra of Mg_2AlO calcined at 100 and 300 °C, respectively, upon the adsorption of CO. Fig. 13(a) presents four main absorption bands. The band at 2170–2190 cm^{-1} is typically attributed to the adsorption of CO on the support oxide [44,45]. Therefore, the absorption band at 2174 cm^{-1} was assigned to the adsorption of CO on Mg_2AlO(100). Two bands at 2361 and 2341 cm^{-1} were assigned to the adsorption of CO_2 on Mg_2AlO(100) [50–52]. The absorption band at 3726 cm^{-1} was assigned to OH groups on Mg_2AlO(100) [53,54]. It is noticed that the intensity of the absorption band at 2173 cm^{-1} increased with time on stream and then was unchanged after the reaction for 15 min. On the other hand, the intensity of the absorption band at 3726 cm^{-1} decreased with time on stream and remained constant after the reaction for 15 min. The intensity of bands at 2340 and 2361 cm^{-1}, assigned to the absorption of CO_2, was initially large and then decreased gradually with time on stream. Furthermore, no apparent absorption band was detected in the carbonate region

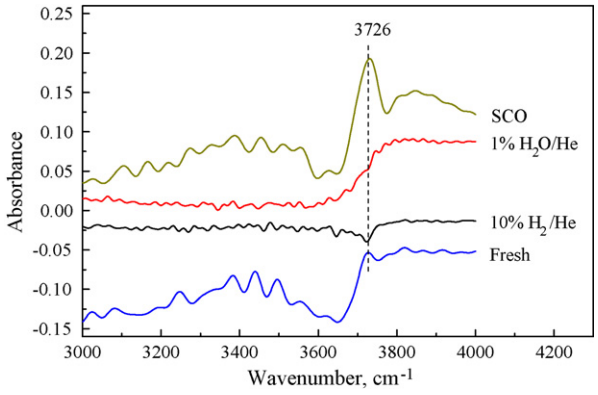

Fig. 12. In situ DR-FTIR spectra of 2%Au/Mg_2AlO(100) under various pretreatment conditions.

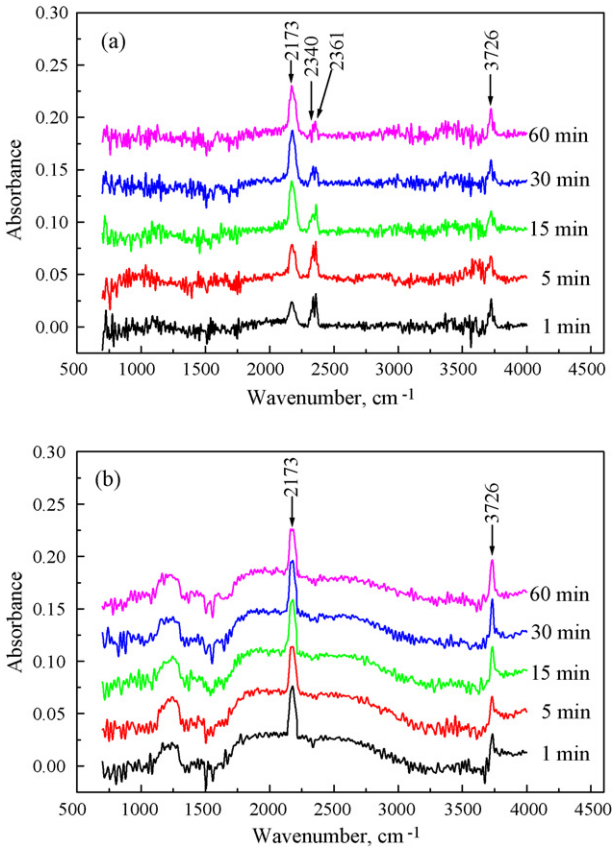

Fig. 13. In situ DR-FTIR spectra of (a)Mg_2AlO(100) and (b) Mg_2AlO(300) under the stream of 10%CO/He (50 cm^3/min) at room temperature.

(1000–1800 cm^{-1}). This phenomenon is explained by the fact that a substantial amount of CO_2 was produced in the initial stage of the reaction between CO and active OH groups on Mg_2AlO(100). After 5 min of the reaction, some weakly adsorbed CO_2 was flushed out by the continuous stream and the intensity of the CO_2 absorption band decreased gradually with time on stream.

Fig. 13(b) shows the absorption spectra of Mg_2AlO(300) upon the adsorption of CO. An absorption band at 2173 cm^{-1} reveals a steady change in intensity with time on stream. No absorption band was observed at 2361 or 2341 cm^{-1}, indicating that no significant CO_2 had been generated. The absorption bands at 1223–1360 cm^{-1} was attributed to the CO_3^{2-} that penetrated from the interlayer of Mg_2AlO(300) during calcination [55]. The absorption band at 3726 cm^{-1} was associated with the inert OH groups on Mg_2AlO calcined at 300 °C [55]. Undoubtedly, the formation of CO_2 in an oxygen-free environment resulted from the reaction between CO and the active OH groups on Mg_2AlO calcined at 100 °C.

Fig. 14(a) and (b) shows the in situ DR-FTIR spectra of 2%Au/Mg_2AlO(100) calcined at 100 and 300 °C, respectively, upon the adsorption of CO in the absence of oxygen. A comparison with the spectra in Fig. 13(a) indicated that Fig. 14(a) showed two new absorption bands at 2116 and 2131 cm^{-1}. The band at 2116 cm^{-1} is assigned to the adsorption of CO on Au^0, whereas that at 2131 cm^{-1} is assigned to the adsorption of CO on Au^{3+} [44–47]. Notably, the intensities of the absorption bands at 2340 and 2361 cm^{-1} increased with time on stream and remained constant after 30 min of reaction. However, the intensity of the absorption band at 3726 cm^{-1} decreased and remained constant after 30 min of the reaction. Au^0 sites are expected to favor CO adsorption; CO reacts with Au^{3+}–OH to form the carboxylate group Au^{3+}–COOH, which

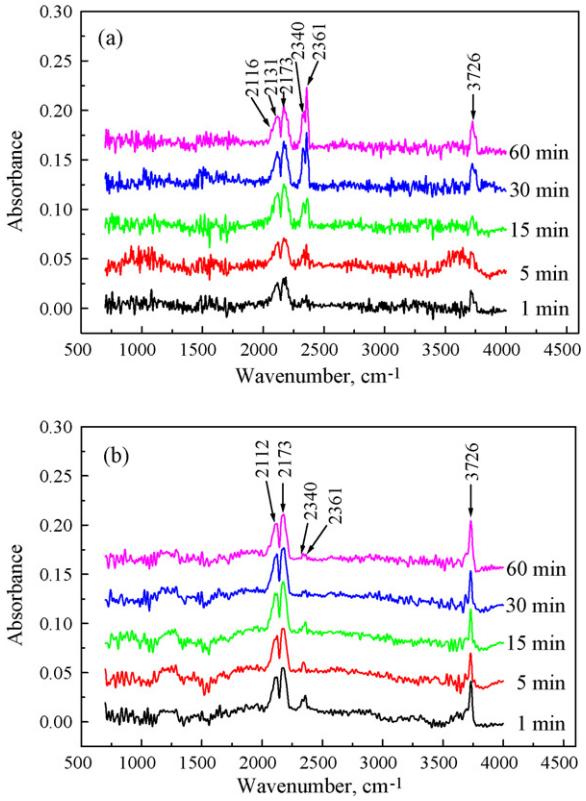

Fig. 14. In situ DR-FTIR spectra of 2%Au/$Mg_2AlO(100)$ calcined at (a) 100 °C and (b) 300 °C under the stream of 10%CO/He (50 cm^3/min) at room temperature.

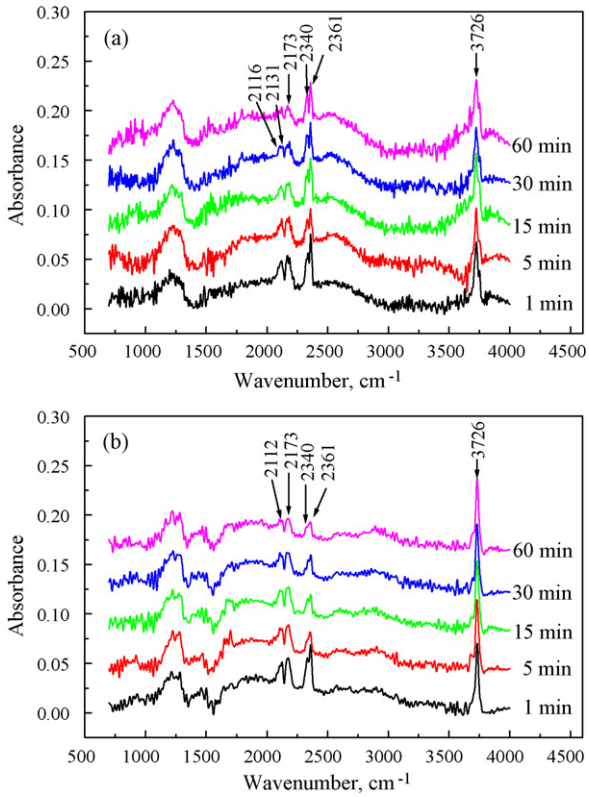

Fig. 15. In situ DR-FTIR spectra of 2%Au/$Mg_2AlO(100)$ calcined at (a) 100 °C and (b) 300 °C under the stream of 2%CO/2%O_2/He (50 cm^3/min) at room temperature.

decomposes to form CO_2. In the mean time, the carboxylate group in the vicinity of Au and $Mg_2AlO(100)$ may also react with the active OH group on $Mg_2AlO(100)$ to form CO_2 and H_2O. H_2O is also capable of replenishing the OH groups on the support as well as Au^{3+}. No obvious absorption band in the carbonate region (1000–1800 cm^{-1}) was observed. Fig. 14(b) displays the in situ DR-FTIR spectra of 2%Au/$Mg_2AlO(100)$ catalysts calcined at 300 °C upon the adsorption of CO. The intensity of the absorption band at 2173 cm^{-1} remained constant as the time on stream increased. Only weak absorption bands at 2340 and 2361 cm^{-1} were observed, and their intensities decreased with time on stream. A comparison with the spectra in Fig. 13(b) indicates that the intensity of the absorption band at 1250 cm^{-1} is weakened. It could be speculated that the trace amount of CO_2 was originated from the decomposition of CO_3^{2-}. Obviously, the oxygen that formed CO_2 from the CO that was adsorbed on Au was contributed by the OH groups on Au and Mg_2AlO for 2%Au/$Mg_2AlO(100)$ calcined at 100 °C. Furthermore, the CO adsorbed on Au was more likely than that adsorbed on the support to react to form CO_2.

Fig. 15(a) shows the in situ DR-FTIR spectra of 2%Au/$Mg_2AlO(100)$ calcined at 100 °C upon the adsorption of CO in the presence of oxygen. The absorption intensities at 2116, 2131 and 2173 cm^{-1} for CO on Au/Au^{3+} and Mg_2AlO, respectively, were significantly weaker than those in Fig. 14(a), and decreased with time. The intensities at 2340 and 2361 cm^{-1} for CO_2 on the catalyst were initially strong and unchanged. The bicarbonate species, evidenced by the absorption band at 1223 cm^{-1}, appeared in the presence of oxygen. These results are explained by the following mechanism. The adsorbed CO of Au^0–CO reacted with the hydroxyl group of Au^{3+}–OH to form the carboxylate group Au^{3+}–COOH which then reacted with the adsorbed oxygen, Au^0–O, to form a bicarbonate intermediate (1223 cm^{-1}), and subsequently decomposed into CO_2 and an OH group. Fig. 15(b) shows the in situ DR-FTIR spectra of 2%Au/$Mg_2AlO(100)$ calcined at 300 °C. The absorption intensities at 2340 and 2361 cm^{-1} for CO_2 on the catalyst were initially strong, and decreased with time, becoming much weaker than those in Fig. 15(a), indicating that less CO_2 was produced during the time on stream. Clearly, the in situ DR-FTIR and XPS spectra of the 2%Au/$Mg_2AlO(100)$ calcined at 100 °C provided evidence of its high activity in CO oxidation [7] and CO selective oxidation. The oxidized states on gold species and active hydroxyl groups on $Mg_2AlO(100)$ are responsible for the high activity of 2%Au/$Mg_2AlO(100)$ calcinated at 100 °C through the synergistic effects.

3.4.2. *In situ DR-FTIR study of SOC reaction*

In situ DR-FTIR analyses were conducted to understand the activation of the 2%Au/Mg_2AlO catalyst during the selective oxidation of CO. Fig. 16 shows the in situ DR-FTIR spectra of 2%Au/Mg_2AlO that is exposed to a reactant stream of 1%CO/1%O_2/50%H_2/48%He at various temperatures. The absorption intensity of the OH group at about 3733 cm^{-1} increased with the temperature to a maximum at 45 °C. The absorption of CO_2 at 2340 and 2361 cm^{-1} was then highest in intensity. This phenomenon is consistent with the complete conversion of CO at about 45 °C for CO selective oxidation. These results demonstrate that the generation of CO_2 may be related to the formation of the OH groups during the reaction. It is worth noting that the two absorption bands at 1090 and 860 cm^{-1} were attributed to the peroxide species [56]. They may be the ozonide reaction intermediate generated from the reaction of gaseous O_2 with surface O^- from OH decomposition. Another in situ DR-FTIR analysis of the 2%Au/Mg_2AlO catalyst (Fig. 17) was performed in 10%CO/He without oxygen. After 1 min of the reaction, absorption bands of CO_2 at 2340 and 2361 cm^{-1} were observed. The absorption

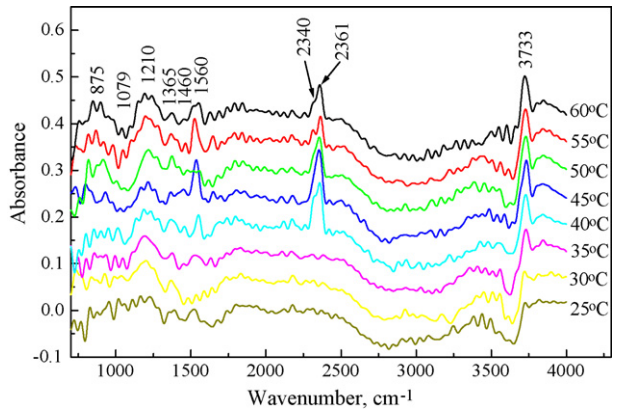

Fig. 16. In situ DR-FTIR spectra of 2%Au/Mg_2AlO under the stream of 1%CO/1%O_2/50%H_2/48%He (100 cm^3/min) at different reaction temperatures.

band of the OH group on Mg_2AlO at 3733 cm^{-1} assumed a negative intensity and fluctuated between the zero intensity of the baseline and negative intensity during the course of the process. This phenomenon is explained by the consumption of OH groups and the replenishment of OH groups from H_2O during the reaction. In the absence of oxygen, CO_2 is formed in a reaction between CO and OH groups. The OH group on Mg_2AlO may participate in CO oxidation. The results of XPS and in situ DR-FTIR analyses demonstrate the mechanism of CO oxidation as follows:

$$Au^0 + CO \rightarrow Au^0 \cdots CO \quad (1)$$

$$Au^0 \cdots CO + Au^{3+} \cdots OH \rightarrow Au^0 + Au^{3+} \cdots COOH \quad (2)$$

$$2Au^0 + O_{2(g)} \rightarrow 2Au^0 \cdots O \quad (3)$$

$$Au^{3+} \cdots COOH + Au^0 \cdots O \rightarrow Au^{3+} \cdots OH + Au^0 + CO_2 \quad (4a)$$

$$Au^{3+} \cdots COOH + S \cdots OH \rightarrow Au^{3+} + CO_2 + S \cdots OH_2 \quad (4b)$$

CO is adsorbed on Au^0 (1) and reacts with Au^{3+}–OH to form the carboxylate group (2), which is adsorbed on the periphery of Au and the Mg_2AlO support. Oxygen on Au^0 dissociates to form Au^0–O (3). The carboxylate group reacts with the oxygen of Au^0–O to form the bicarbonate intermediate which then dissociates into CO_2 and OH radical (4a). Simultaneously, the carboxylate group may also react with the OH group on Mg_2AlO to form CO_2 and H_2O (4b). The OH group on Mg_2AlO can be replenished by H_2O and adsorbed on Au^{3+}. Step (4b) of this mechanism can be used to elucidate the enhancement of the catalytic activity of the 2%Au/Mg_2AlO catalyst as it undergoes selective CO oxidation. The adsorption of the OH groups on Au^{3+} and their replenishment by H_2O did not change the stability of Au^{3+} on the 2%Au/Mg_2AlO catalyst, maintaining the Au^{3+}/Au^0 ratio that is suitable for the reaction.

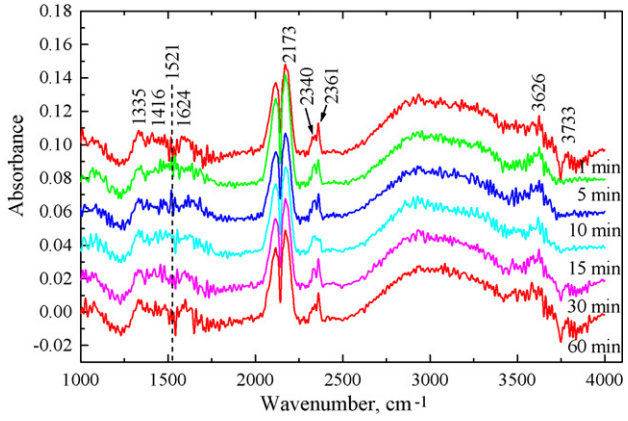

Fig. 17. In situ DR-FTIR spectra of 2%Au/Mg_2AlO (after pretreatment) under the stream of 10%CO/He (50 cm^3/min) at room temperature.

4. Conclusion

Gold was dispersed and stabilized on a solid base of Mg_xAlO hydrotalcite using a modified DP method to obtain a favorable catalyst for the selective oxidation of CO. The pH and the $HAuCl_4$ concentration in the initial gold solution, and the Mg/Al molar ratio of Mg_xAlO affected the pH of the final gold solution and determined the actual gold loading of the catalyst. The calcination temperature of the Mg_xAlO support and the catalyst dominated the ratio of gold states (Au^{3+}/Au^0) on the catalyst. The optimal catalyst 2%Au/Mg_2AlO(100) was obtained with the preparation parameters as follows: (1) 1×10^{-3} M $HAuCl_4$, (2) pH 2 (without adjusting pH) in the initial solution, (3) Mg/Al = 2 (Mg_2AlO) calcined at 100 °C as a support, and (4) 2%Au/Mg_2AlO catalyst calcined at 100 °C. Pretreatment of 2%Au/Mg_2AlO under the stream of CO/O_2/He at about 45 °C enhanced its reactivity. The oxidized states on the gold species and the active hydroxyl groups on Mg_2AlO are the two causes of the favorable reactivity of 2%Au/Mg_2AlO through synergistic effects.

Acknowledgements

The authors would like to thank the Ministry of Economic Affairs of the Republic of China, Taiwan, for financially supporting this research under MOEA 95-EC-17-A-09-S1-022. The assistance of Professor Wei-Lin Dai of the Department of Chemistry, Fudan University, Shanghai, China, with the XPS analyses is sincerely appreciated.

References

[1] R.J.H. Grisel, B.E. Nieuwenhuy, J. Catal. 199 (2001) 48–59.
[2] M.M. Schubert, V. Plzak, J. Garche, R.J. Behm, Catal. Lett. 76 (2001) 143–150.
[3] A. Luengnaruemitchai, S. Osuwan, E. Gulari, Int. J. Hydrogen Energy 29 (2004) 429–435.
[4] C. Rossignol, S. Arrii, F. Morfin, L. Piccolo, V. Caps, J.L. Rousset, J. Catal. 230 (2005) 476–483.
[5] D. Gavril, A. Georgaka, V. Loukopoulos, G. Karaiskakis, B.E. Nieuwenhuy, Gold Bull. 39 (2006) 192–199.
[6] T.V.W. Janssens, A. Carlsson, A. Puig-Molina, B.S. Clausen, J. Catal. 240 (2006) 108–113.
[7] C.T. Chang, B.J. Liaw, C.T. Huang, Y.Z. Chen, Appl. Catal. A: Gen. 332 (2007) 216–224.
[8] L. Fan, N. Ichikuni, S. Shinazu, T. Uematsu, Appl. Catal. A: Gen. 246 (2003) 87–95.
[9] J.D. Grunwaldt, C. Kiener, C. Wogerbauer, A.J. Baiker, J. Catal. 181 (1999) 223–232.
[10] R. Zanella, L. Delannoy, C. Louis, Appl. Catal. A: Gen. 291 (2005) 62–72.
[11] S. Ivanova, C. Petit, V. Pitchon, Appl. Catal. A: Gen. 267 (2004) 191–201.
[12] A.I. Kozlov, A.P. Kozlova, H. Lin, Y. Iwasawa, Appl. Catal. A: Gen. 182 (1999) 9–28.
[13] A. Wolf, F. Schuth, Appl. Catal. A: Gen. 226 (2002) 1–13.
[14] I. Dobrosz, K. Jiratova, V. Pitchon, J.M. Rynkowski, J. Mol. Catal. A: Chem. 234 (2005) 187–197.
[15] F. Moreau, G.C. Bond, A.O. Taylor, J. Catal. 231 (2005) 105–114.
[16] S. Ivanova, V. Pitchon, C. Petit, H. Herschbach, A.V. Dorsselaer, E. Leize, Appl. Catal. A: Gen. 298 (2006) 203–210.
[17] W.C. Li, M. Comotti, F. Schüth, J. Catal. 237 (2006) 190–196.
[18] M.S. Chen, D.W. Goodman, Catal. Today 111 (2006) 22–33.
[19] M. Mavrikakis, P. Stoltze, J.K. Norskov, Catal. Lett. 64 (2000) 101–106.
[20] N. Weiher, E. Bus, L. Delannoy, C. Louis, D.E. Ramaker, J.T. Miller, J.A.V. Bokhoven, J. Catal. 240 (2006) 100–107.
[21] Z.P. Liu, X.Q. Gong, J. Kohanoff, C. Sanchez, P. Hu, Phys. Rev. Lett. 91 (2003) 266102-1–266102-4.
[22] A.I. Kozlov, A.P. Kozlova, K. Asakura, Y. Matsui, T. Kogure, T. Shido, Y. Iwasawa, J. Catal. 196 (2000) 56–65.
[23] J.C. Fierro-Gonzalez, B.C. Gate, J. Phys. Chem. B 107 (2003) 2242–2248.
[24] R.P. Nnikrishnan, D. Sarojini, Appl. Catal. A: Gen. 299 (2006) 266–273.
[25] S.T. Daniells, A.R. Overweg, M. Makkee, J.A. Moulijn, J. Catal. 230 (2005) 52–65.
[26] M.M. Schubert, S. Hackenberg, A.C.V. Veen, M. Muhler, V. Plzak, R.J. Behm, J. Catal. 197 (2001) 113–122.

[27] N. Lopez, T.V.W.B.S. Clausen, Y. Xu, M. Marvrikakis, T. Bligaard, J.K. Norskov, J. Catal. 223 (2004) 232–235.
[28] N.A. Hodge, C.J. Kiely, R. Whyman, M.R.H. Siddiqui, G.H. Hutchings, Q.A. Pankhurst, P.E. Wanger, R.R. Rajaram, S.E. Golunski, Catal. Today 72 (2002) 133–144.
[29] E.D. Park, J.S. Lee, J. Catal. 186 (1999) 1–11.
[30] A.M. Visco, F. Neri, G. Neri, A. Donato, C. Milone, S. Galvagno, Phys. Chem. Chem. Phys. 1 (1999) 2869–2878.
[31] M. Date, M. Haruta, J. Catal. 201 (2001) 221–224.
[32] D.A.H. Cunningham, W. Vogel, M. Haruta, Catal. Lett. 63 (1999) 43–47.
[33] M. Date, M. Okumura, S. Tsubota, M. Haruta, Angew. Chem. Int. Ed. 43 (2004) 2129–2132.
[34] M. Harauta, N. Yamada, T. Kobayashi, S. Iijima, J. Catal. 115 (1989) 301–309.
[35] D. Andreeva, V. Idakiev, T. Tabakova, L. Ilieva, P. Falaras, A. Bourlinos, A. Travlos, Catal. Today 72 (2002) 51–57.
[36] A. Knell, P. Barnickel, A. Baiker, A. Wokaun, J. Catal. 137 (1992) 306–321.
[37] J.L. Margitfalvi, A. Fasi, M. Hegeds, F. Lonyi, S. Gbolos, N. Bogdanchikova, Catal. Today 72 (2002) 157–169.
[38] S.J. Lee, A. Gavriilidis, J. Catal. 206 (2002) 305–313.
[39] L.M. Molina, B. Hammer, Phys. Rev. Lett. 90 (2003), 206102-1-206102-4.
[40] K. Jiratova, P. Cuba, F. Kovanda, L. Hilaire, V. Pitchon, Catal. Today 76 (2002) 43–49.
[41] S. Narayanan, K. Krishna, Appl. Catal. A: Gen. 174 (1998) 221–229.
[42] F. Kovanda, K. Jirátová, J. Rymeš, D. Koloušek, Appl. Clay Sci. 18 (2001) 71–80.
[43] A. Corma, V. Fornes, F. Rey, J. Catal. 148 (1994) 205–212.
[44] F. Boccuzzi, A. Chiorino, M. Manzoli, D. Andreeva, T. Tabakova, J. Catal. 188 (1999) 176–185.
[45] J.D. Grunwaldt, A. Baiker, J. Phys. Chem. B 103 (1999) 1002–1012.
[46] J.L. Margitfalvi, M. Hegedus, A. Szegedi, I. Sajo, Appl. Catal. A: Gen. 272 (2004) 87–97.
[47] E.G. Szabo, A. Tompos, M. Hegedus, A. Szegedi, J.L. Margitfalvi, Appl. Catal. A: Gen. 320 (2007) 114–121.
[48] G.C. Bond, D.T. Thompson, Gold Bull. 33 (2000) 41–51.
[49] C.K. Costello, J.H. Yang, H.Y. Law, Y. Wang, J.N. Lin, L.D. Marks, M.C. Kung, H.H. Kung, Appl. Catal. A: Gen. 243 (2003) 15–24.
[50] M.A. Bollinger, M.A. Vannice, Appl. Catal. B: Environ. 8 (1996) 417–443.
[51] H. Liu, A.I. Anguelina, P. Kozlova, T. Shido, Y. Iwasawa, Phys. Chem. Chem. Phys. 1 (1999) 2851–2860.
[52] N.M. Gupta, A.K. Tripathi, Gold Bull. 34 (2001) 120–128.
[53] B. Aeijelts Averink Silberova, G. Mul, M. Makkee, J.A. Molijn, J. Catal. 243 (2006) 171–182.
[54] J.D. Grunwaldt, M. Maciejewski, O.S. Becker, P. Fabrizioli, A. Baiker, J. Catal. 186 (1999) 458–469.
[55] D. Tichit, M.H. Lhouty, A. Guida, B.H. Chiche, F. Figueras, A. Auroux, D. Bartalini, E. Garrone, J. Catal. 151 (1995) 50–59.
[56] I.M. Mellor, A. Burrows, S. Coluccia, J.S.J. Hargreaves, R.W. Joyner, C.J. Kiely, G. Marra, M. Stockenhuber, W.M. Tang, J. Catal. 234 (2005) 14–23.